

Title	Improved efficiency of anaerobic digestion through direct interspecies electron transfer at mesophilic and thermophilic temperature ranges
Authors	Lin, Richen;Cheng, Jun;Ding, Lingkan;Murphy, Jerry D.
Publication date	2018-05-30
Original Citation	Lin, R., Cheng, J., Ding, L. and Murphy, J. D. (2018) 'Improved efficiency of anaerobic digestion through direct interspecies electron transfer at mesophilic and thermophilic temperature ranges', Chemical Engineering Journal, In Press, doi: 10.1016/j.cej.2018.05.173
Type of publication	Article (peer-reviewed)
Link to publisher's version	<a href="https://www.sciencedirect.com/science/article/pii/S1385894718309975">https://www.sciencedirect.com/science/article/pii/S1385894718309975</a> - 10.1016/j.cej.2018.05.173
Rights	© 2018 Elsevier B.V. All rights reserved. This manuscript version is made available under the CC-BY-NC-ND 4.0 license. - <a href="http://creativecommons.org/licenses/by-nc-nd/4.0/">http://creativecommons.org/licenses/by-nc-nd/4.0/</a>
Download date	2023-05-05 08:39:44
Item downloaded from	<a href="http://hdl.handle.net/10468/6254">http://hdl.handle.net/10468/6254</a>



# UCC

**University College Cork, Ireland**  
Coláiste na hOllscoile Corcaigh

## Accepted Manuscript

Improved efficiency of anaerobic digestion through direct interspecies electron transfer at mesophilic and thermophilic temperature ranges

Richen Lin, Jun Cheng, Lingkan Ding, Jerry D. Murphy

PII: S1385-8947(18)30997-5  
DOI: <https://doi.org/10.1016/j.cej.2018.05.173>  
Reference: CEJ 19189

To appear in: *Chemical Engineering Journal*

Received Date: 26 March 2018  
Revised Date: 25 May 2018  
Accepted Date: 29 May 2018

Please cite this article as: R. Lin, J. Cheng, L. Ding, J.D. Murphy, Improved efficiency of anaerobic digestion through direct interspecies electron transfer at mesophilic and thermophilic temperature ranges, *Chemical Engineering Journal* (2018), doi: <https://doi.org/10.1016/j.cej.2018.05.173>



This is a PDF file of an unedited manuscript that has been accepted for publication. As a service to our customers we are providing this early version of the manuscript. The manuscript will undergo copyediting, typesetting, and review of the resulting proof before it is published in its final form. Please note that during the production process errors may be discovered which could affect the content, and all legal disclaimers that apply to the journal pertain.

# Improved efficiency of anaerobic digestion through direct interspecies electron transfer at mesophilic and thermophilic temperature ranges

Richen Lin<sup>a, b</sup>, Jun Cheng<sup>c\*</sup>, Lingkan Ding<sup>c</sup>, Jerry D. Murphy<sup>a, b, d</sup>

<sup>a</sup> *MaREI Centre, Environmental Research Institute, University College Cork, Cork, Ireland*

<sup>b</sup> *School of Engineering, University College Cork, Cork, Ireland*

<sup>c</sup> *State Key Laboratory of Clean Energy Utilization, Zhejiang University, Hangzhou 310027, China*

<sup>d</sup> *International Energy Agency Bioenergy Task 37 "Energy from Biogas"*

## Abstract

Direct interspecies electron transfer (DIET) in microbial communities plays a significant role in improving efficiency of biomethane production from anaerobic digestion. In this study, the impacts of conductive graphene on mesophilic and thermophilic anaerobic digestion (MAD and TAD) were comparatively assessed using the model substrate ethanol. The maximum electron transfer flux for graphene-based DIET was calculated at mesophilic and thermophilic temperatures (35 °C and 55 °C).

Biomethane potential results showed that the addition of graphene (1.0 g/L) significantly enhanced biomethane production rates by 25.0% in MAD and 26.4% in TAD. The increased biomethane

---

\* Corresponding author: Prof. Dr. Jun Cheng, State Key Laboratory of Clean Energy Utilization, Zhejiang University, Hangzhou 310027, China. Tel.: +86 571 87952889; fax: +86 571 87951616. E-mail: juncheng@zju.edu.cn

production was accompanied with enhanced ethanol degradation. The theoretical calculation for maximum DIET flux showed that graphene-based DIET in MAD (76.4 mA) and TAD (75.1 mA) were at the same level, which suggests temperature might not be a significant factor affecting DIET. This slight difference was ascribed to the different Gibbs free energy changes of the overall DIET reaction ( $\text{CH}_3\text{CH}_2\text{OH} + 1/2\text{CO}_2 \rightarrow 1/2\text{CH}_4 + \text{CH}_3\text{COO}^- + 5\text{H}^+$ ) in MAD and TAD. Microbial analysis revealed that the dominant microbes in response to graphene addition were distinctly different between MAD and TAD. The results indicated that the bacteria of *Levilinea* dominated in MAD, while *Coprothermobacter* dominated in TAD. The abundance of archaeal *Methanobacterium* decreased, while *Methanosaeta* increased with increasing temperature.

**Keywords:** Graphene; ethanol; mesophilic / thermophilic digestion; interspecies electron transfer.

## Nomenclature

### Abbreviations

[Acetate]	acetic acid concentration	MIET	mediated interspecies electron transfer
BMP	biomethane potential	MSW	municipal solid waste
CSTR	continuous stirred-tank reactor	n	mole electron per reaction
DIET	direct interspecies electron transfer	OTU	operational taxonomic unit
d	distance between cells	pCH <sub>4</sub>	methane partial pressure
[Ethanol]	ethanol concentration	pCO <sub>2</sub>	carbon dioxide partial pressure
E <sub>Met</sub>	redox potential of ethanol oxidation reaction	R	universal gas constant
E <sub>Ace</sub>	redox potential of carbon dioxide reduction reaction	R <sub>m</sub>	peak gas production rate
ΔE	maximum redox potential of overall reaction	S <sub>conduit</sub>	cross sectional area of the electron conduit
F	Faraday's constant	T	reaction temperature
GAC	granular activated carbon	TAD	thermophilic anaerobic digestion
ΔG <sup>0</sup>	standard Gibbs free energy change	T <sub>m</sub>	gas production peak time
ΔG'	Gibbs free energy change	TS	total solid
H <sub>m</sub>	maximum gas yield potential	UASB	up-flow anaerobic sludge blanket
i	direct electron transfer flux	VFA	volatile fatty acid
MAD	mesophilic anaerobic digestion	VS	volatile solid
		<i>Greek letters</i>	
		λ	lag-phase time
		σ	electrical conductivity of graphene

## 1. Introduction

Fossil fuel consumption is still the dominant source of global energy, despite the significant contribution to the rise in greenhouse gas emissions and the decrease in urban air quality. The EU has committed to achieving at least 20% renewable energy share of gross energy consumption by 2020, rising to at least 27% by 2030 [1]. The production of biogas as a renewable energy carrier via anaerobic

digestion has proven to be highly effective in mitigation of greenhouse gas emissions through the combination of carbon efficient waste treatment and displacement of fossil fuels [2-5].

The International Energy Agency (IEA) Energy Technology Perspectives 2017 report outlines the requirement for sustainable bioenergy use in sectors with limited decarbonisation options [6]. Transport is the least decarbonized sector when compared to electricity and heat. This is exemplified by the recast Renewable Energy Directive that requires 3.6% advanced biofuels by 2030 [1]. Biogas production from wastes and algae can fill this target when upgraded to biomethane. The European Biogas Association state that in 2015, there were 459 biogas-upgrading plants in operation producing 1,230 M Nm<sup>3</sup> of biomethane equivalent to approximate 45.5 TJ [7]. The IEA suggest that biomethane for transport should rise to 3.74 EJ by 2040 [6]. For such a remarkable rise in output, there is significant requirement for optimisation of the operational conditions of the anaerobic digestion process including for temperature range and the microbial communities.

Anaerobic digestion is generally carried out under either mesophilic (35–40 °C) or thermophilic (55–70 °C) conditions by a variety of microorganisms, involving syntrophic bacteria and methanogenic archaea. Mesophilic anaerobic digestion (MAD) has the general advantage of higher stability performance during operation [8]. MAD produces a relatively lower volume of biogas with lower loading capacity [9]. In contrast, thermophilic anaerobic digestion (TAD) allows for higher organic loading rate, enhanced hydrolysis rate, and higher biogas production rate [10-14]. However, the

application of TAD can be limited by low system stability, long start-up phase and long microbial acclimation phase.

The potential for inefficiency and instability of anaerobic digestion fundamentally arises from the microbial process of interspecies electron transfer. The challenge on how to improve electron transfer efficiency is critical to enhance biogas production and optimize the anaerobic digestion system. The predominant understanding of interspecies electron transfer in anaerobic digestion was based on mediated interspecies electron transfer (MIET) via hydrogen and formate [15, 16]. MIET is thermodynamically feasible only at very low metabolite concentration (especially hydrogen) [17]. Recent findings revealed that direct interspecies electron transfer (DIET) via biological pili, mineral, or shuttle molecules is a more efficient alternative to MIET [18, 19]. It is hypothesized that DIET does not require the multiple enzymatic steps to produce hydrogen as an electron carrier between bacteria and archaea [18]. To date, much attention has been devoted to assessing the effects of adding conductive carbon-based materials on either MAD or TAD. Conductive materials, such as granular activated carbon (GAC), biochar, carbon cloth, graphite, magnetite, and carbon-based nanomaterials have been employed mostly in MAD to assess the digestion performance [19-21]. Results from previous studies indicated that conductive materials could act as an electron conduit for efficient direct electron transfer between syntrophic partners, leading to enhanced MAD performance [21, 22]. For example, Lee et al. demonstrated that GAC addition in MAD resulted in a 1.8 fold higher biomethane production rate than

that without GAC addition [22]. Further microbial analysis revealed that the exoelectrogens (such as *Geobacter*) and hydrogenotrophic methanogens (such as *Methanospirillum* and *Methanolinea*) were greatly enriched after GAC addition [22]. Zhao et al. found that conductive carbon cloth could assist in resisting the acidic impacts in anaerobic digestion [20]. This was due to the fact that the dominant working mode for the syntrophic metabolism shifted from MIET to DIET [20]. In comparison to the research on MAD, there is only limited knowledge on the effects of carbon-based materials on TAD in terms of biogas production kinetics and microbial communities. MAD and TAD are populated with entirely different microorganisms. Chen et al. reported that only 10% of the microbial community in mesophilic sludge were thermophiles [23]. The temperature change from the mesophilic to thermophilic condition may result in a substantial microbial shift, thus leading to a long acclimation time [13]. Yan et al. demonstrated that conductive carbon nanotube could contribute to a more stable TAD performance and lower volatile fatty acids (VFAs) accumulation [10]. Microbial analysis revealed that it is highly possible that *Caloramator* and *Methanosaeta*/*Methanosarcina* established DIET, through employing carbon nanotube as an electron conduit. Thus, it is assumed that temperature might be a critical factor affecting the mechanism of DIET. Nonetheless, the understanding of how conductive materials affect DIET both thermodynamically and phylogenetically needs to be improved.

To the best knowledge of the authors, there is a clear research gap on investigation of the difference between DIET-based MAD and TAD. The innovation in this study is that it is the first to



compare the effects of conductive nanomaterial (in this case graphene) on the performance of MAD and TAD, including the biomethane production and the shift of microbial communities. In particular, this study provides the clue on how temperature would affect the maximum DIET flux based on thermodynamic calculations. The objective of this study is to assess the biomethane production from a model substrate (in this case ethanol) in MAD and TAD in the presence of graphene. In detail, it calculates the theoretical maximum DIET flux via graphene in MAD and TAD, and compares the shift of bacterial and archaeal communities in response to graphene.

## **2. Material and Methods**

### **2.1. Inoculum and material**

The original inoculum for biomethane potential (BMP) assays of both MAD and TAD was sourced from lab-scale continuous stirred-tank reactors (operated at 35 °C), processing various substrates such as grass, dairy slurry and seaweed. Then the inoculum for MAD was kept at 35 °C in a water bath, while being fed once a week with cellulose as a carbon source at an organic loading rate of 1.0 g/L/d. To acclimatize the original inoculum for use in TAD, the inoculum was kept at 45°C in a water bath for two weeks while being fed with cellulose (1.0 g/L/d). Then the temperature in the water bath was adjusted to 55 °C for further four weeks acclimation. The acclimatized inocula at 35 °C and 55 °C were used in MAD and TAD. The total solid (TS) content in MAD and TAD is determined as 3.5

wwt% and 2.5 wwt%. The volatile solid (VS) content in MAD and TAD is determined as 2.1 wwt% and 1.3 wwt%.

Graphene nanoplatelets were purchased from Sigma–Aldrich and used in the experiments without further purification or modification. The nanoplatelets typically consist of aggregates of sub-micron platelets that have a particle diameter of less than 2  $\mu\text{m}$  and a typical particle thickness of a few nanometers. The used graphene nanoplatelets show a very high surface area (500  $\text{m}^2/\text{g}$ ). The electrical conductivity of graphene was determined typically as 850 S/cm in a previous study [24].

## 2.2. Biomethane potential assays

Batch experiments of MAD and TAD were carried out in triplicate in two AMPTS II systems (Bioprocess Control, Sweden), as illustrated in Fig. 1. Each BMP system has the capacity to accommodate 15 glass bottles, which serve as the batch anaerobic digester. Each glass bottle has a total volume of 650 mL with a working volume of 400 mL. Four experimental groups were designed for both MAD and TAD assays in terms of graphene concentrations (0, 0.5, 1.0 and 2.0 g/L). To minimize the effect of the carryover of inocula on digestion, a blank group without substrate (only inoculum) was operated in both MAD and TAD assays.

In BMP assays for MAD, 1.5 g of ethanol as a substrate were added to each glass bottle. A certain amount of MAD inoculum containing 3.0 g of VS was subsequently added to each bottle. Different

amounts of graphene were separately added into glass bottles to meet the designed graphene concentrations. The initial pH was adjusted to  $7.5 \pm 0.1$  through use of HCl and NaOH solution. The final liquid volume in each bottle was adjusted to 400 mL by using distilled water. Afterwards, all glass bottles were sealed with rubber stoppers, purged with nitrogen gas for 5 min, and maintained at  $35 \pm 1.0$  °C. Carbon dioxide in the produced biogas was removed by passing the biogas through 3 M sodium hydroxide solution. The gas flow was measured and the volume was automatically normalized to standard conditions (0 °C, 1 atm) by the AMPST II system. In BMP assays for TAD, the TAD inoculum was used in the BMP experiments. All the bottles were kept at  $55 \pm 1.0$  °C in water bath during digestion. The other procedures were the same as MAD assays.

## **2.3. Analytic methods**

### **2.3.1. Chemical analyses**

The TS, VS and ash contents of the inocula were analyzed by using the standard method of drying of the sample for 24 h at 105 °C and subsequent heating for 2 h at 550 °C. The concentrations of ethanol and acetic acid were analyzed on a gas chromatography system (GC; Agilent 7890A, USA) equipped with a flame ionization detector and a DB-FFAP column. The temperatures of injection port and flame ionization detector were both set at 250 °C. The initial column temperature was set at 75 °C, increased to 180 °C at a heating rate of 16 °C/min, and then held for 1.15 min. For the determination of

ethanol and acetic acid, the liquid samples were first centrifuged at 5000 rpm for 5 min and then adjusted with orthophosphoric acid to pH 2.0. The quantification of each component was determined by a standard solution, containing 0.06 v/v% of ethanol and 0.06 v/v% of acetic acid. All of the trials and measurements were conducted in triplicate, and the results were expressed as mean  $\pm$  standard deviation.

### **2.3.2. Microbial community analysis**

The samples of digestate were taken at the end of the digestion period to identify the microbial communities in both MAD and TAD assays. The digestate samples were rinsed with phosphate-buffered saline and then centrifuged for 10 min at 4 °C. The pretreated samples were stored at -20 °C until further use. The microbial community was characterized using high-throughput 16S rRNA pyrosequencing as described in a previous study [25]. DNA extraction was performed following the manufacturer's protocol (E.Z.N.ATM Mag-Bind Soil DNA Kit, Omega Bio-Tec, China). The extracted samples were amplified in two independent polymerase chain reactions (PCR) with primers spanning the V3-V4 hypervariable region of the 16S rRNA gene. PCR products were checked in 2% agarose gel to determine the success of amplification. Samples were pooled together in equal proportions based on their molecular weight and DNA concentrations. Then the samples were purified using calibrated Ampure XP beads. The pooled and purified PCR product was processed by sequencing

on the Miseq sequencing platform (Illumina, USA) by Sangon Biotech (Sangon Biotech Shanghai, China). Operational taxonomic units (OTUs) were defined by clustering at 3% divergence (97% similarity). Final OTUs were taxonomically classified using BLASTN against a curated database derived from RDP [26].

## 2.4. Calculations

### 2.4.1 Kinetic model and statistical analysis

Biomethane yields of MAD and TAD were simulated by the modified Gompertz equation (Eq. 1), and the kinetic parameters ( $H_m$ , maximum biomethane yield potential, mL/g;  $R_m$ , peak biomethane production rate, mL/g/h;  $\lambda$ , lag-phase time of biomethane production, h; and  $T_m$ , peak time of biomethane production, h) were calculated using Origin 8.5 software.

$$H = H_m \exp \left\{ -\exp \left[ \frac{R_m e}{H_m} (\lambda - t) + 1 \right] \right\} \quad (1)$$

Statistical analysis of variance (one-way ANOVA) was carried out using Origin 8.5 software to test the impact of graphene addition on biomethane production from MAD and TAD. The value of  $p < 0.05$  was considered to be statistically significant.

### 2.4.2 Calculation of theoretical direct interspecies electron transfer flux

The maximum electron transfer flux for graphene-based DIET in MAD and TAD was calculated

based on Ohm's law and Nernst equation as described in Eq. 2 [17, 25].

$$i = \sigma \cdot \frac{S_{conduit}}{d} \cdot (E_{Met} - E_{Ace}) \quad (2)$$

where  $i$  (A) is the direct electron transfer flux,  $\sigma$  is the electrical conductivity of graphene,  $S_{conduit}$  is the cross sectional area of the electron conduit (assuming as a cuboid shape with a thickness of 16 nm and a length of 2  $\mu$ m),  $d$  is the distance between cells (assuming as 0.5  $\mu$ m),  $E_{Met}$  is the redox potential of the ethanol oxidation reaction, and  $E_{Ace}$  is the redox potential of the carbon dioxide reduction reaction.

$\Delta E = E_{Met} - E_{Ace}$  can be determined using the following equation (Eq. 3).

$$\Delta E = E_{Met} - E_{Ace} = \frac{\Delta G'}{nF} \quad (3)$$

where  $\Delta E$  (V) is the maximum redox potential of the overall reaction for ethanol oxidation and carbon dioxide reduction,  $n$  is mole electron per reaction, and  $F$  is the Faraday's constant.  $\Delta G'$  can be calculated according to Eq. 4.

$$\Delta G' = \Delta G^{0'} + RT \ln \frac{[Acetate] \cdot pCH_4^{1/2}}{[Ethanol] \cdot pCO_2^{1/2}} \quad (4)$$

where  $\Delta G^{0'}$  (kJ/mol) is the standard Gibbs free energy change per reaction,  $R = 8.315$  J/(mol·K),

[Acetate] and [Ethanol] are the concentrations of acetic acid and ethanol in the reaction,  $pCH_4$  and

$pCO_2$  are the concentrations of methane and carbon dioxide in the reaction, and  $T$  (K) is the reaction

temperature (308 K or 328 K). The values of  $\Delta G^{0'}$  at different temperatures are determined based on

previous reported data [27, 28]. The concentrations of reactants and products used in calculations are as

follows: [Acetate] = 2.50 g/L, [Ethanol] = 1.88 g/L,  $pCH_4$  = 0.6 atm, and  $pCO_2$  = 0.2 atm.

### 3. Results and discussion

#### 3.1. Effects of graphene addition on biomethane production in MAD and TAD

The effects of graphene addition on biomethane yield and production rate in MAD are illustrated in Fig. 2 a and b, respectively. Ethanol was employed as the model substrate because it only contains two carbon atoms with acetic acid as metabolic product. In MAD, the biomethane yield without graphene addition was 121.3 mL/g after 108 h of digestion. The addition of graphene in MAD resulted in the increase of biomethane yield, as shown in Fig. 2 a. The highest biomethane yield of 138.0 mL/g ( $p < 0.05$ ) was achieved with the addition of 1.0 g/L graphene in MAD, corresponding to a value of 13.8% higher as compared to the control. It was noted that even though graphene addition of 1.0 g/L resulted in the highest biomethane production, the lower graphene loading of 0.5 g/L also improved biomethane production to a level of 133.9 mL/g, which is only 3.0% lower than the highest value. This result suggested that the threshold concentration of graphene for improving anaerobic digestion might be even lower than 0.5 g/L. Previous study showed a clear positive effect of graphene on anaerobic digestion of glucose [29]. Even with an addition of 30 mg/L graphene, the methane production rate increased by 17.0%. As shown in Fig. 2 a, the biomethane yield did not alter significantly when further increasing graphene addition to 2.0 g/L. This was likely due to the fact that excess addition of graphene could lead to the microbial inhibition effect caused by the penetration of nanoparticles through the cell

membrane.

As shown in Fig. 2 b, the peak biomethane production rate was obtained as 4.8 mL/g/h without graphene addition. With the addition of 1.0 g/L graphene, the peak production rate accordingly increased to 6.0 mL/g/h ( $p < 0.05$ ). Furthermore, the time for peak production rate was greatly reduced from 54 h to 42 h. These results suggested that graphene played a significant role in enhancing MAD performance. This can be possibly attributed to the improved microbial electron transfer efficiency in the presence of highly conductive graphene, serving as an electron conduit among microbes. Graphene nanomaterials have unique physicochemical properties, including exceptionally high electric conductivity, large surface area and good mechanical strength. These properties have led to novel or improved applications in biotechnological research, such as microbial fuel cells and anaerobic digestion [21, 30]. Previous studies have revealed that graphene could promote DIET and enable an enhanced anaerobic digestion in mesophilic temperature. Tian et al. showed that graphene functioned as an electric conduit rather than an electron shuttle (such as quinones) between bacteria and archaea in anaerobic digestion of glucose [29]. As a result, graphene (120 mg/L) had significantly positive effects on biomethane production rate, which increased by 51.4% as compared to no graphene addition [29].

Similarly, Lin et al. demonstrated that 1.0 g/L of graphene addition in mesophilic digestion resulted in a much higher biomethane yield than 20.0 g/L of less conductive activated charcoal [25]. This result indicated that graphene nanomaterial has superior advantage over low conductive material in



promoting anaerobic digestion.

The kinetic parameters of biomethane production in MAD were simulated by the modified Gompertz equation, as shown in Table 1. The kinetics were evaluated in terms of the biomethane yield potential ( $H_m$ ), peak biomethane production rate ( $R_m$ ), lag phase time ( $\lambda$ ) and peak time ( $T_m$ ). The simulation results confirmed that graphene addition promoted MAD performance. The peak biomethane production rate increased by between 8.2–12.2% through addition of graphene. The lag phase time of MAD was reduced by 20.8% with 1.0 g/L graphene addition. In a similar way, the peak time of MAD was reduced by 16.7% with the addition of 1.0 g/L graphene. These results suggested that the addition of graphene had an evident influence on the kinetics of biomethane production in MAD.

One proposed hypothesis on enhanced DIET mechanism was that carbon based materials could function as novel electron shuttles rather than electron conduits. The electron shuttles could transfer electrons outside the cells through the reducing and oxidizing cycle. Extracellular quinones, such as anthraquinone-2,6-disulfonate (AQDS) were widely suggested as efficient electron shuttles between microorganisms and extracellular electron acceptors [31, 32]. However, a previous study demonstrated that adding AQDS at various concentrations did not stimulate methanogenesis [29]. The failure of AQDS to replicate graphene stimulation on methanogenesis indicated that graphene was not an AQDS equivalent, suggesting that graphene did not function as electron shuttles. Similarly, Liu et al. also demonstrated that AQDS could not replace activated carbon to stimulate interspecies electron transfer

[33]. These results led to the conclusion that graphene likely acts as an electron conduit transferring electrons between cells rather than as electron shuttles.

To investigate the difference between MAD and TAD, this study further assessed the performance of TAD in the presence of graphene. The effects of graphene addition on biomethane yield and production rate in TAD are shown in Fig. 3 a and b, respectively. The biomethane yield of 141.7 mL/g was obtained in TAD without graphene addition. Different amount of graphene additions contributed to enhanced TAD performance to different extents as can be seen in Fig. 3 a. The addition of 1.0 g/L graphene resulted in the highest biomethane yield of 148.7 mL/g ( $p < 0.05$ ), corresponding to an enhancement of 4.9% in comparison to no graphene addition. As shown in Fig. 3b, the peak biomethane production rates in the presence of graphene increased to 8.8–11.0 mL/g/h as compared to 8.7 mL/g/h in the absence of graphene. In addition, the time for peak production rate was reduced from 60 h to 48–54 h. These results demonstrated that the performance of TAD was greatly improved by graphene addition. It is conceivable that graphene can promote DIET in TAD in a similar way to MAD with graphene acting as electron conduit. Only a few studies investigated the effects of conductive materials on anaerobic digestion in thermophilic temperature range. Yan et al. found that conductive materials (such as carbon nanotube and activated carbon) shortened the start-up period of thermophilic digestion [10]. The addition of conductive material could assist in establishing DIET and accelerating the start-up period by reducing the accumulation of intermediates, mitigating inhibition induced from

unbalanced reaction kinetics, and improving the methanogenesis process. The presence of biochar in TAD could dramatically shorten the lag time of methane production and increase the methane production rate from co-digestion of food waste and waste activated sludge [34]. The higher buffer capacity and large specific surface area of biochar could promote microorganism growth and alleviate the accumulation of VFAs. Furthermore, the electron exchange in syntrophic oxidation of butyrate and acetate as intermediate products was significantly facilitated by biochar [34].

The kinetic parameters of biomethane production in TAD are shown in Table 1. Similar to MAD, the presence of graphene in TAD also enhanced the kinetics of digestion performance. The peak biomethane production rate of TAD greatly increased by 9.3-67.4% in the presence of graphene. The lag phase time of TAD was reduced by 24.8%, and the peak time was accordingly reduced by 22.8% with the addition of 1.0 g/L graphene. The kinetic analysis demonstrated that suitable addition of graphene could enable an improved TAD performance.

### **3.2. Effects of graphene addition on substrate degradation in anaerobic digestion**

As a typical electron-donating source, ethanol can be readily consumed by the syntrophy of acidogenic bacteria and methanogenic archaea. Firstly, ethanol will be used by acidogenic bacteria to produce acetic acid and release hydrogen/electrons through either MIET or DIET routes. Secondly, the produced hydrogen/electrons can be utilized by methanogenic archaea for carbon dioxide reduction.

Acetoclastic methanogens can further degrade acetic acid into methane. Table 2 presents the Gibbs free energy change for ethanol conversion to methane at the temperatures of 25 °C, 35 °C and 55 °C. From a thermodynamic perspective, DIET can provide additional energy benefits to the syntrophic partners because metabolite (such as hydrogen) generation and diffusion is unnecessary [35]. Taking the example at 25 °C (biological standard condition), the start-up process of ethanol degradation via DIET ( $\Delta G^{\circ'} = -149.6$  kJ/mol) is thermodynamically more favorable than that via MIET ( $\Delta G^{\circ'} = +9.7$  kJ/mol).

The effects of graphene addition (1.0 g/L) on ethanol conversion in MAD are shown in Fig. 4 a. The concentrations of ethanol and acetate were monitored during digestion. Ethanol was continuously degraded while generating acetate during MAD. The presence of graphene enhanced the degradation of ethanol and acetate production. With the addition of 1.0 g/L graphene, 50.0% of ethanol was consumed in the first 48 h of digestion, whereas only 28.9% of ethanol was consumed without graphene addition. This result was in agreement with a previous study, showing that the kinetic degradation of ethanol was improved by almost 30% in the presence of graphene in anaerobic digestion [25]. The acetate concentration gradually increased with the degradation of ethanol in MAD. The highest acetate concentration of 4.3 g/L was observed at 96 h in the presence of 1.0 g/L graphene, as compared to acetate concentration of 3.2 g/L in the absence of graphene. These results indicated that graphene is capable of promoting syntrophic reactions between acidogenic bacteria and methanogenic archaea,

which in turn facilitates substrate degradation and utilization for enhanced syntrophic mutualism. A similar result was observed in a previous study [36], in which a much faster substrate utilization was achieved with the addition of carbon nanotube. This result could be attributed to the enhanced anaerobic microbial activity in the presence of carbon nanotube [36]. It is noteworthy that a great amount of acetate remained after MAD. This is due to the rapid accumulation of acetic acid, resulting in rather low pH (approximate 5.5) and resultant stress on digestion process.

The effects of graphene addition (1.0 /L) on ethanol conversion in TAD can be found in Fig. 4 b. The trend of the conversion of ethanol and acetate in TAD are similar to that of MAD. With the addition of 1.0 g/L graphene, 54.9% of ethanol was consumed in the first 48 h of TAD, while only 12.4% of ethanol was consumed without graphene addition. In accordance with the ethanol degradation, acetate reached a higher concentration at 96 h in the presence of graphene than that without graphene addition.

### **3.3. Effects of graphene addition on microbial community in anaerobic digestion**

The microbial communities after MAD and TAD were analyzed using 16S rRNA sequencing for better understanding of bacterial and archaeal responses to graphene addition. For both MAD and TAD, three groups of digestate samples including original inoculum (not digested), digestate without graphene addition, and digestate with 1.0 g/L of graphene addition were analyzed (see Table 3).

### 3.3.1 Effect of graphene addition on bacterial community

The statistics of the bacterial community in terms of microbial richness and diversity are listed in Table 3. For each group in MAD and TAD, three indicators including OTU numbers, Chao richness estimator and Shannon's diversity index are presented. The analysis results showed that the OTU number of MAD inoculum was the highest (853) as compared to those (676 and 734) after digestion regardless of graphene addition, suggesting that the bacterial richness decreased with the operational time of digestion. This result can be ascribed to the assimilation effect of ethanol, which selectively enriched strains favoring ethanol metabolism in digestion. In MAD, the bacterial richness in ethanol digestion after graphene addition increased as indicated by the higher OTU and Chao index. A higher Shannon index was also obtained after graphene addition, suggesting a higher bacterial diversity. These results implied that adding graphene in MAD could increase the bacterial richness and diversity, contributing to a better digestion performance. A similar trend of bacterial richness (OTU and Chao) and diversity (Shannon) was found in TAD. The indexes of OTU, Chao and Shannon all increased in response to graphene addition in TAD. All the Coverage values approaching to 1.00 in both MAD and TAD indicated that the coverage was sufficient to capture most of the microbial diversity.

The improved biomethane production from digestion was fundamentally ascribed to the syntrophic activity of electron-producing acidogens and electron-consuming methanogens. Therefore, understanding the microbial shift in response to graphene will help to reveal the DIET mechanism. The

dominant bacteria at genus level were further assessed to give better understanding of microbial shift, as shown in Table 4. In the initial seed sludge of MAD, *Levilinea* (18.4%), *Bacteroides* (12.7%) and *Clostridium XIVa* (5.9%) genera were the dominant part of the bacterial community. *Levilinea* are recognized as anaerobic fermentative bacteria, which are capable of fermenting sugars and amino acids into hydrogen, acetic and lactic acids [37]. *Bacteroides* are reported to be common in mesophilic anaerobic digesters where they are able to degrade a wide range of macromolecules, such as starch and cellulose [38]. *Clostridium XIVa* are common strains involved in fermentation converting carbohydrates to hydrogen along with the production of volatile fatty acids (VFAs, such as acetate and butyrate) [39].

After the MAD of ethanol without graphene, the abundance of *Levilinea* remarkably increased to 29.0%, while that of *Bacteroides* decreased to 5.9%. With the addition of graphene in MAD, *Levilinea* (18.3%) and *Bacteroides* (13.3%) accounted for the dominant bacterial groups. Notably, the abundance of *Bacteroides* was greatly enriched from 5.9% (no graphene addition) to 13.3% in the presence of graphene, suggesting its potential role in DIET during MAD.

The bacterial compositions of the initial TAD inoculum were distinctly different from those of MAD inoculum. In the original TAD inoculum, *Coprothermobacter* (27.0%), *Acinetobacter* (16.3%) and *Clostridium III* (11.9%) were the most abundant fermentative genera, accounting for 55.2% of the overall bacterial abundance. *Coprothermobacter* are identified as hydrogen-producing strains in thermophilic digesters, and may have the function of oxidizing acetate in syntrophic relation with

methanogenic archaea [40]. The species of *Coprothermobacter proteolyticus* was predominantly present in TAD using grass as the substrate [41]. The bacterial abundance significantly shifted to *Coprothermobacter* (44.8%) and *Defluviitoga* (26.7%) after TAD of ethanol without graphene addition. Comparatively, *Defluviitoga* were further enriched to 33.3% after graphene addition, while *Coprothermobacter* decreased to 36.1%. *Defluviitoga* genus consists of one known species *Defluviitoga tunisiensis*, which is a thermophilic (55 °C as the optimum) sulfur-reducing bacteria [42]. *D. tunisiensis* is capable of degrading a variety of sugars to acetate, hydrogen, and carbon dioxide. A previous study reported that the genus *Defluviitoga* was the most dominant bacterium in thermophilic digestion systems fed with protein-rich wastes such as stillage and food waste, but the exact roles of this bacteria in those systems were not determined [42]. Given that *Defluviitoga* was drastically enriched in TAD with graphene, it was conceivable that *Defluviitoga* played a potentially positive role in DIET.

### 3.3.2 Effect of graphene addition on archaeal community

The statistics of the archaeal community in terms of microbial richness and diversity are listed in Table 3. Three indicators including OTU numbers, Chao richness estimator and Shannon's diversity index are provided for each group in MAD and TAD. Similar to the bacterial results, the archaeal OTU number of MAD inoculum was the highest (96) as compared to those (74 and 66) after digestion regardless of graphene addition, suggesting that the archaeal richness decreased with the operational



time of digestion of ethanol. This was attributed to the fact that ethanol was used as the sole carbon source in digestion. The archaeal richness after graphene addition in MAD was found to have decreased as indicated by the lower OTU and Chao index. However, a higher Shannon index of 1.05 was obtained after graphene addition as compared to that of 0.91 without graphene addition. The higher Shannon index indicated a higher archaeal diversity due to graphene addition. Unlike the results from MAD, the archaeal richness (OTU and Chao) and diversity (Shannon) in TAD increased in response to graphene addition. These results suggested that graphene addition could lead to different microbial statistics in MAD and TAD.

For better evaluation of the functions of microbial communities, the genus level of archaeal communities in MAD and TAD is shown in Table 5. In the initial seed sludge of MAD, the genera of *Methanobacterium* (64.3%) and *Methanosaeta* (27.2%) contributed to the dominant part of the archaeal community. *Methanobacterium* are conventionally recognized as hydrogen-consuming methanogens, converting carbon dioxide and hydrogen into methane [43, 44]. *Methanosaeta* are mainly acetate-consuming methanogens which cleave acetate into methane and carbon dioxide [43]. Recently, some species of *Methanosaeta* (such as *M. harundinacea*) have been found capable of receiving electrons via DIET for carbon dioxide reduction into methane [16]. When ethanol was used as substrate in MAD, *Methanobacterium* was enriched to 88.8%, whereas *Methanosaeta* decreased to 8.4%. By adding graphene in MAD, *Methanobacterium* (83.0%) and *Methanosaeta* (9.9%) were still the major

group. However, an obvious enrichment of *Methanosarcina* (6.2%) known as the most metabolically diverse methanogens were detected, indicating the potential change of methane producing pathway in MAD. Previous studies have demonstrated that archaea *Methanosarcina* are capable of receiving electrons from electro-active bacteria (such as *Geobacter*) to perform DIET as the syntrophy pathway in methanogenic communities [16, 45].

The major archaeal groups in the initial TAD inoculum were found as *Methanobacterium* (39.8%) *Methanosarcina* (30.1%) and *Methanosaeta* (26.1%). The archaeal community was acclimatized to *Methanobacterium* (52.8%) and *Methanosaeta* (38.2%) in TAD with ethanol as substrate. When adding graphene in TAD, *Methanobacterium* were further enriched to 60.4%. Notably, an enrichment of *Methanothermobacter* (3.2%) was detected in TAD in response to graphene addition.

### 3.4 Microbial network for ethanol degradation in MAD and TAD

The microbial networks of key bacteria and archaea involved in MAD and TAD with graphene addition are illustrated in Fig. 5. The complete conversion of ethanol to methane in MAD and TAD requires effective syntrophy between acidogenic bacteria and methanogenic archaea. The acidogenic bacteria are responsible for converting ethanol to acetic acid and producing electrons (or in the form of hydrogen). Methanogenic archaea are capable of converting acetic acid, carbon dioxide, and electrons to methane through three major pathways, comprising of acetoclastic methanogenesis,

hydrogenotrophic methanogenesis, and DIET methanogenesis. However, the microbial communities involved in MAD and TAD are considerably different as temperature is a significant factor affecting the microbial mechanism of ethanol degradation in digestion.

Ethanol was mainly degraded by acidogenic bacteria including *Levilinea* (18.3%) and *Bacteroides* (13.3%) in graphene added MAD, as presented in Fig. 5 a. The intermediate products such as acetic acid, and hydrogen (or protons and electrons), could be further utilized by acetoclastic, hydrogenotrophic, and DIET methanogens through three major pathways. Acetic acid was utilized by *Methanosaeta* (9.9%) to produce methane and carbon dioxide in MAD. Carbon dioxide could be reduced to methane by *Methanobacterium* (83.0%) and *Methanosarcina* (6.2%) through the hydrogenotrophic pathway. Alternatively, some species of *Methanobacterium* and *Methanosarcina* are capable of directly receiving electrons to reduce carbon dioxide through DIET methanogenesis. For instance, Rotaru et al. demonstrated the successful DIET mode for electron flow during mesophilic digestion [16]. Further research proved that *Methanosaeta harundinacea* and *Geobacter metallireducens* could stoichiometrically convert ethanol to methane through DIET via electrically conductive pili [16]. *Geobacter* have been known as “exoelectrogen”, which have ability to perform DIET in MAD. However, in this study, the abundance of *Geobacter* was not detectable in digestate after digestion regardless of graphene addition. A similar study has observed that microbial granules almost devoid of *Geobacter* species were also able to use conductive mineral material to perform DIET

[46]. Dang et al. also found that *Geobacter* species were not enriched with conductive material addition in digestion of complex organic waste, suggesting that other microorganisms might participate in DIET [47].

As shown in Fig. 5 b, the microbial network of key bacteria and archaea involved in TAD were greatly different from that in MAD. The acidogenic bacteria in TAD were mainly composed of *Coprothermobacter* (36.1%) and *Deftluviitoga* (33.1%), which are responsible for ethanol conversion to acetic acid, and hydrogen (or protons and electrons). These generated intermediates require efficient utilization by methanogens to keep them at low concentrations due to the thermodynamic limits [17]. Acetic acid could be readily used by *Methanosaeta* (28.6%) through acetoclastic pathway. Hydrogen could be employed for carbon dioxide reduction by *Methanobacterium* (60.4%), *Methanosarcina* (4.4%) and *Methanothermobacter* (3.2%). It was assumed that some species of the above methanogens are potentially active for DIET methanogenesis in TAD. Yan et al. proposed that *Caloramator* and *Methanosaeta*/*Methanosarcina* could establish syntrophic DIET in thermophilic digestion, via adopting conductive materials (such as carbon nanotube) as electron conduit [10].

### 3.5. Maximum electron transfer flux for graphene-based DIET in MAD and TAD

Interspecies electron transfer between electron-producing acetogens and electron-consuming methanogens in anaerobic digestion can rely on either DIET or MIET (with hydrogen as an electron

carrier). DIET can proceed via biological electrical connections or a combination of biological and non-biological electron transfer materials (such as graphene, biochar and ferric oxide). Non-biological, conductive materials, including mineral particles and carbon materials, can enhance DIET in syntrophic methanogenic cultures by serving as electron conduits. Previous studies have demonstrated that DIET can sustain much higher electron flux than MIET in mesophilic digestion [17, 25]. By using a reaction-diffusion-electrochemical approach, Storck et al. revealed that MIET is limited by the mediator concentration gradient at which reactions are still thermodynamically feasible, whereas DIET is limited by the redox cofactor (for example, cytochromes) activation losses [48].

However, the understanding on how different temperatures would affect the maximum DIET flux remained limited. To quantitatively compare the DIET flux in MAD and TAD, the simplified calculations based on Ohm's law and Nernst equation were proposed. It was assumed that the electrons are released from the ethanol oxidation reaction ( $\text{CH}_3\text{CH}_2\text{OH} + \text{H}_2\text{O} \rightarrow \text{CH}_3\text{COO}^- + 5\text{H}^+ + 4\text{e}^-$ , see Equation 2 Table 2) in MAD and TAD. Then the electrons are directly transferred to methanogens via conductive graphene. Carbon dioxide can be reduced to methane by methanogens through the electron-consuming reaction ( $4\text{H}^+ + 4\text{e}^- + 1/2\text{CO}_2 \rightarrow 1/2\text{CH}_4 + \text{H}_2\text{O}$ , see Equation 4 Table 2). Overall, the maximum driving force for electron transfer is given by the redox potential ( $\Delta E$ ) of the sum reaction ( $\text{CH}_3\text{CH}_2\text{OH} + 1/2\text{CO}_2 \rightarrow 1/2\text{CH}_4 + \text{CH}_3\text{COO}^- + \text{H}^+$ ). The Gibbs free energy changes for each reaction can be separately determined at the temperatures of 35 °C and 55 °C. Thus, the calculated  $\Delta E$

for MAD and TAD was determined as 140.5 mV and 138.1 mV, respectively. By further using Ohm's law, the resulting maximum DIET flux via graphene for MAD and TAD was obtained as 76.4 mA and 75.1 mA, respectively. These values are comparable to the DIET flux achieved under mesophilic condition from previous studies, in which the maximum electron flux through DIET was proved to be much higher than that through MIET [17, 25]. The DIET fluxes obtained from MAD and TAD were at the same level, which suggests temperature might not be a significant factor affecting DIET flux. This slight difference was mainly achieved because of the thermodynamic advantage of DIET reaction in MAD, in which the value of Gibbs free energy change is more negative than that in TAD (-55.7 kJ/mol versus -54.8 kJ/mol, see Table 2).

### 3.6. Implications of conductive materials on anaerobic digestion

The present study demonstrated that conductive graphene could enhance the performance of both MAD and TAD, in which the peak biomethane production rate and substrate degradation significantly increased. Previous studies have suggested that conductive materials are capable of stimulating DIET, resulting in enhanced biomethane production. By using GAC, Liu et al. successfully established DIET in co-culture of pili-deficient *Geobacter metallireducens* and *Methanosarcina barkeri* [33]. The demonstration of DIET in microbial co-cultures has led to increased attention in engineering applications of anaerobic digesters. Significant research efforts have been focused on promoting DIET

in methanogenic digesters by adding conductive materials.

A summary of carbon-based conductive materials used for improving DIET in mesophilic and thermophilic digestion is presented in Table 6. Carbon-based materials such as activated carbon, biochar, carbon cloth, graphite, and carbon-based nanomaterials have shown great potential in promoting digestion performance at both mesophilic and thermophilic temperatures (33–55 °C). The methane production rate could be enhanced by 1.9%–100% with addition of different types of conductive materials (Table 6). The hypothesis is that conductive materials can act as electron conduit and may allow microbial cells to conserve more energy. GAC is a porous carbon material, which was commonly used for microbial support material in bioreactors. Due to the high surface area and electrical conductivity, GAC has been widely employed to stimulate DIET in mesophilic and thermophilic digesters. Zhao et al. demonstrated that GAC could promote DIET and improve the syntrophic metabolism of propionate/butyrate in the ethanol-stimulated microbial communities in MAD [49]. Similarly, Lee et al. concluded that GAC supplementation created an environment for enriching the microbes involved in DIET [22]. As a result, the reactor supplemented with GAC showed an increase in methane production rate by 77.6% as compared to that without GAC. The high specific area and porous structure of GAC provided an ideal condition for microbial attachment, contributing to higher methane production rate. Yan et al. showed that GAC could promote the start-up of thermophilic digestion, as evidenced by low VFA accumulation, high methane production rate, and more robust

responses against hydrogen inhibition [10]. Other traditional carbon-based materials (such as biochar, carbon cloth and carbon felt) have also been assessed for improving digestion performance in terms of methane yield, methane production rate and other kinetic parameters. Biocompatible nanomaterials (such as graphene and carbon nanotube) are gaining heightened attention and have been integrated with various biological applications [30, 50]. These nanomaterials have unique physicochemical properties including the exceptionally high surface area, electron mobility, and thermal conductivity. Lin et al. and Tian et al. found that mesophilic digestion performance could be greatly improved by suitable addition of graphene [25, 29]. However, these research outputs also highlighted that excess addition of graphene could result in inhibition to microorganisms in digestion. More stable performance and lower VFAs accumulation in TAD were observed in the presence of carbon nanotubes [10]. Microbial analysis revealed that it is highly possible that *Caloramator* and *Methanosaeta*/*Methanosarcina* established DIET, through employing carbon nanotubes as electron conduit [10].

Anaerobic digestion has proven to be an effective strategy to recovery energy from biomass wastes [2, 51]. However, process instability and inefficiency have occurred in traditional anaerobic digesters due to the unbalanced relationship and lack of efficient syntrophy between acidogenic bacteria and methanogenic archaea. The establishment of DIET is an emerging approach that has great potential to significantly improve digestion performance. The findings of this study suggests that the combination of conductive materials and anaerobic digestion would benefit the biomethane yield and



production rate. This could lead to a new process integration that couples the mesophilic/thermophilic anaerobic digestion with the cost-effective conductive biochar (potentially derived from pyrolysis or gasification). Future work is required to demonstrate the feasibility and sustainability of such bioenergy system. Reutilization of conductive materials should be considered in future systems to make the process economically viable.

#### 4. Conclusions

Findings from this research suggested that graphene could significantly improve the performance of MAD and TAD, presumably because of the establishment of direct interspecies electron transfer (DIET) via graphene. The addition of graphene (1.0 g/L) resulted in improved biomethane production rates by 25.0% in MAD and 26.4% in TAD, respectively. The degradation of ethanol was simultaneously improved in digestion. Thermodynamic calculations showed that graphene-based DIET in MAD (76.4 mA) and TAD (75.1 mA) could sustain the DIET flux to a similar level. The slight difference was ascribed to the thermodynamic advantage of the DIET reaction at mesophilic temperature. Further microbial analysis revealed that the dominant syntrophic bacteria and methanogenic archaea involved in MAD and TAD were distinctly different, suggesting that diverse temperature-dependent microbes might participate in DIET. When it is considered that the market for biomethane as a transport fuel needs to yield 3.74 EJ by 2040, the improved efficiency of ca. 25% in

anaerobic digestion systems through DIET can significantly reduce the infrastructural investment

required to meet this target.

## Acknowledgements

This collaborative Irish Chinese study was co-funded by Science Foundation Ireland (SFI) through the Centre for Marine and Renewable Energy (MaREI) under Grant No. 12/RC/2302, and by the National key research and development program-China (2016YFE0117900). This work was also funded by Zhejiang Provincial key research and development program-China (2017C04001), industrially co-funded by ERVIA and Gas Networks Ireland (GNI) through the Gas Innovation Group. Dr. Richen Lin gratefully acknowledges the support from the European Union's Horizon 2020 research and innovation programme under the Marie Skłodowska-Curie grant agreement No. 797259.

## References

1. *Proposal for a DIRECTIVE OF THE EUROPEAN PARLIAMENT AND OF THE COUNCIL on the promotion of the use of energy from renewable sources (recast), COM/2016/0767 final/2 - 2016/0382 (COD).*
2. Batstone, D.J. and B. Viridis, *The role of anaerobic digestion in the emerging energy economy.* Current Opinion in Biotechnology, 2014. **27**: 142-149.

3. Czyrnek-Delêtre, M.M., S. Rocca, A. Agostini, J. Giuntoli, and J.D. Murphy, *Life cycle assessment of seaweed biomethane, generated from seaweed sourced from integrated multi-trophic aquaculture in temperate oceanic climates*. *Applied Energy*, 2017. **196**: 34-50.
4. Salman, C.A., S. Schwede, E. Thorin, and J. Yan, *Enhancing biomethane production by integrating pyrolysis and anaerobic digestion processes*. *Applied Energy*, 2017. **204**: 1074-1083.
5. Shen, Y., J.L. Linville, M. Urgan-Demirtas, R.P. Schoene, and S.W. Snyder, *Producing pipeline-quality biomethane via anaerobic digestion of sludge amended with corn stover biochar with in-situ CO<sub>2</sub> removal*. *Applied Energy*, 2015. **158**: 300-309.
6. International Energy Agency (IEA) *Energy Technology Perspectives 2017*. available in: <http://www.iea.org/etp2017/summary/>.
7. European Biogas Association. 2016. *6th edition of the Statistical Report on European anaerobic digestion industry and markets*.
8. Meng, Y., C. Jost, J. Mumme, K. Wang, and B. Linke, *An analysis of single and two stage, mesophilic and thermophilic high rate systems for anaerobic digestion of corn stalk*. *Chemical Engineering Journal*, 2016. **288**: 79-86.
9. Choong, Y.Y., K.W. Chou, and I. Norli, *Strategies for improving biogas production of palm oil mill effluent (POME) anaerobic digestion: A critical review*. *Renewable and Sustainable*

- Energy Reviews, 2018. **82**: 2993-3006.
10. Yan, W., N. Shen, Y. Xiao, Y. Chen, F. Sun, V. Kumar Tyagi, and Y. Zhou, *The role of conductive materials in the start-up period of thermophilic anaerobic system*. Bioresource Technology, 2017. **239**: 336-344.
11. Wu, L.-J., A. Higashimori, Y. Qin, T. Hojo, K. Kubota, and Y.-Y. Li, *Comparison of hyper-thermophilic–mesophilic two-stage with single-stage mesophilic anaerobic digestion of waste activated sludge: Process performance and microbial community analysis*. Chemical Engineering Journal, 2016. **290**: 290-301.
12. Voelklein, M., D. Rusmanis, and J. Murphy, *Increased loading rates and specific methane yields facilitated by digesting grass silage at thermophilic rather than mesophilic temperatures*. Bioresource technology, 2016. **216**: 486-493.
13. Zhu, X., P.G. Kougias, L. Treu, S. Campanaro, and I. Angelidaki, *Microbial community changes in methanogenic granules during the transition from mesophilic to thermophilic conditions*. Applied Microbiology and Biotechnology, 2017. **101**: 1313-1322.
14. Zhu, X., L. Treu, P.G. Kougias, S. Campanaro, and I. Angelidaki, *Converting mesophilic upflow sludge blanket (UASB) reactors to thermophilic by applying axenic methanogenic culture bioaugmentation*. Chemical Engineering Journal, 2018. **332**: 508-516.
15. Kouzuma, A., S. Kato, and K. Watanabe, *Microbial interspecies interactions: recent findings*

- in syntrophic consortia*. Frontiers in Microbiology, 2015. **6**.
16. Rotaru, A.-E., P.M. Shrestha, F. Liu, M. Shrestha, D. Shrestha, M. Embree, K. Zengler, C. Wardman, K.P. Nevin, and D.R. Lovley, *A new model for electron flow during anaerobic digestion: direct interspecies electron transfer to Methanosaeta for the reduction of carbon dioxide to methane*. Energy & Environmental Science, 2014. **7**: 408-415.
  17. Cruz Viggi, C., S. Rossetti, S. Fazi, P. Paiano, M. Majone, and F. Aulenta, *Magnetite Particles Triggering a Faster and More Robust Syntrophic Pathway of Methanogenic Propionate Degradation*. Environmental Science & Technology, 2014. **48**: 7536-7543.
  18. Lovley, D.R., *Live wires: direct extracellular electron exchange for bioenergy and the bioremediation of energy-related contamination*. Energy & Environmental Science, 2011. **4**: 4896-4906.
  19. Lei, Y., L. Wei, T. Liu, Y. Xiao, Y. Dang, D. Sun, and D.E. Holmes, *Magnetite enhances anaerobic digestion and methanogenesis of fresh leachate from a municipal solid waste incineration plant*. Chemical Engineering Journal, 2018. **348**: 992-999.
  20. Zhao, Z., Y. Zhang, Y. Li, Y. Dang, T. Zhu, and X. Quan, *Potentially shifting from interspecies hydrogen transfer to direct interspecies electron transfer for syntrophic metabolism to resist acidic impact with conductive carbon cloth*. Chemical Engineering Journal, 2017. **313**: 10-18.
  21. Barua, S. and B.R. Dhar, *Advances towards understanding and engineering direct interspecies*

- electron transfer in anaerobic digestion*. Bioresource Technology, 2017. **244**: 698-707.
22. Lee, J.-Y., S.-H. Lee, and H.-D. Park, *Enrichment of specific electro-active microorganisms and enhancement of methane production by adding granular activated carbon in anaerobic reactors*. Bioresource technology, 2016. **205**: 205-212.
  23. Chen, M., *Adaptation of mesophilic anaerobic sewage fermentor populations to thermophilic temperatures*. Applied and Environmental Microbiology, 1983. **45**: 1271-1276.
  24. Du, J., L. Zhao, Y. Zeng, L. Zhang, F. Li, P. Liu, and C. Liu, *Comparison of electrical properties between multi-walled carbon nanotube and graphene nanosheet/high density polyethylene composites with a segregated network structure*. Carbon, 2011. **49**: 1094-1100.
  25. Lin, R., J. Cheng, J. Zhang, J. Zhou, K. Cen, and J.D. Murphy, *Boosting biomethane yield and production rate with graphene: The potential of direct interspecies electron transfer in anaerobic digestion*. Bioresource Technology, 2017. **239**: 345-352.
  26. RDP database, Available at <http://rdp.cme.msu.edu/misc/resources.jsp>.
  27. Amend, J.P. and E.L. Shock, *Energetics of overall metabolic reactions of thermophilic and hyperthermophilic Archaea and Bacteria*. FEMS Microbiology Reviews, 2001. **25**: 175-243.
  28. Thauer, R.K., K. Jungermann, and K. Decker, *Energy conservation in chemotrophic anaerobic bacteria*. Bacteriological reviews, 1977. **41**: 100.
  29. Tian, T., S. Qiao, X. Li, M. Zhang, and J. Zhou, *Nano-graphene induced positive effects on*

- methanogenesis in anaerobic digestion*. Bioresource Technology, 2017. **224**: 41-47.
30. ElMekawy, A., H.M. Hegab, D. Losic, C.P. Saint, and D. Pant, *Applications of graphene in microbial fuel cells: The gap between promise and reality*. Renewable and Sustainable Energy Reviews, 2017. **72**: 1389-1403.
31. Xu, J., L. Zhuang, G. Yang, Y. Yuan, and S. Zhou, *Extracellular quinones affecting methane production and methanogenic community in paddy soil*. Microbial ecology, 2013. **66**: 950-960.
32. Amezcuita-Garcia, H.J., J.R. Rangel-Mendez, F.J. Cervantes, and E. Razo-Flores, *Activated carbon fibers with redox-active functionalities improves the continuous anaerobic biotransformation of 4-nitrophenol*. Chemical Engineering Journal, 2016. **286**: 208-215.
33. Liu, F., A.-E. Rotaru, P.M. Shrestha, N.S. Malvankar, K.P. Nevin, and D.R. Lovley, *Promoting direct interspecies electron transfer with activated carbon*. Energy & Environmental Science, 2012. **5**: 8982-8989.
34. Li, Q., M. Xu, G. Wang, R. Chen, W. Qiao, and X. Wang, *Biochar assisted thermophilic co-digestion of food waste and waste activated sludge under high feedstock to seed sludge ratio in batch experiment*. Bioresource Technology, 2018. **249**: 1009-1016.
35. Cheng, Q. and D.F. Call, *Hardwiring microbes via direct interspecies electron transfer: mechanisms and applications*. Environmental Science: Processes & Impacts, 2016. **18**: 968-980.

36. Li, L.-L., Z.-H. Tong, C.-Y. Fang, J. Chu, and H.-Q. Yu, *Response of anaerobic granular sludge to single-wall carbon nanotube exposure*. Water research, 2015. **70**: 1-8.
37. Yamada, T., Y. Sekiguchi, S. Hanada, H. Imachi, A. Ohashi, H. Harada, and Y. Kamagata, *Anaerolinea thermolimos* sp. nov., *Levilinea saccharolytica* gen. nov., sp. nov. and *Leptolinea tardivitalis* gen. nov., sp. nov., novel filamentous anaerobes, and description of the new classes *Anaerolineae* classis nov. and *Caldilineae* classis nov. in the bacterial phylum Chloroflexi. International journal of systematic and evolutionary microbiology, 2006. **56**: 1331-1340.
38. Azizi, A., W. Kim, and J.H. Lee, *Comparison of microbial communities during the anaerobic digestion of Gracilaria under mesophilic and thermophilic conditions*. World Journal of Microbiology and Biotechnology, 2016. **32**: 158.
39. Ferraz Júnior, A.D.N., C. Etchebehere, and M. Zaiat, *High organic loading rate on thermophilic hydrogen production and metagenomic study at an anaerobic packed-bed reactor treating a residual liquid stream of a Brazilian biorefinery*. Bioresource Technology, 2015. **186**: 81-88.
40. Gagliano, M., C. Braguglia, A. Gianico, G. Mininni, K. Nakamura, and S. Rossetti, *Thermophilic anaerobic digestion of thermal pretreated sludge: role of microbial community structure and correlation with process performances*. water research, 2015. **68**: 498-509.
41. Tsapekos, P., P.G. Kougias, L. Treu, S. Campanaro, and I. Angelidaki, *Process performance*



- and comparative metagenomic analysis during co-digestion of manure and lignocellulosic biomass for biogas production. Applied Energy, 2017. 185: 126-135.*
42. Lee, J., G. Han, S.G. Shin, T. Koo, K. Cho, W. Kim, and S. Hwang, *Seasonal monitoring of bacteria and archaea in a full-scale thermophilic anaerobic digester treating food waste-recycling wastewater: correlations between microbial community characteristics and process variables. Chemical Engineering Journal, 2016. 300: 291-299.*
43. Gonzalez-Fernandez, C., B. Sialve, and B. Molinuevo-Salces, *Anaerobic digestion of microalgal biomass: Challenges, opportunities and research needs. Bioresource Technology, 2015. 198: 896-906.*
44. Yin, Q., S. Yang, Z. Wang, L. Xing, and G. Wu, *Clarifying electron transfer and metagenomic analysis of microbial community in the methane production process with the addition of ferroferric oxide. Chemical Engineering Journal, 2018. 333: 216-225.*
45. Rotaru, A.-E., P.M. Shrestha, F. Liu, B. Markovaite, S. Chen, K.P. Nevin, and D.R. Lovley, *Direct interspecies electron transfer between Geobacter metallireducens and Methanosarcina barkeri. Applied and environmental microbiology, 2014. 80: 4599-4605.*
46. Dubé, C.-D. and S.R. Guiot, *Ethanol-to-methane activity of Geobacter-deprived anaerobic granules enhanced by conductive microparticles. Process Biochemistry, 2017. 63: 42-48.*
47. Dang, Y., D.E. Holmes, Z. Zhao, T.L. Woodard, Y. Zhang, D. Sun, L.-Y. Wang, K.P. Nevin,

- and D.R. Lovley, *Enhancing anaerobic digestion of complex organic waste with carbon-based conductive materials*. Bioresource technology, 2016. **220**: 516-522.
48. Storck, T., B. Virdis, and D.J. Batstone, *Modelling extracellular limitations for mediated versus direct interspecies electron transfer*. The ISME journal, 2016. **10**: 621.
49. Zhao, Z., Y. Zhang, Q. Yu, Y. Dang, Y. Li, and X. Quan, *Communities stimulated with ethanol to perform direct interspecies electron transfer for syntrophic metabolism of propionate and butyrate*. Water research, 2016. **102**: 475-484.
50. Khan, M.Z., A.S. Nizami, M. Rehan, O.K.M. Ouda, S. Sultana, I.M. Ismail, and K. Shahzad, *Microbial electrolysis cells for hydrogen production and urban wastewater treatment: A case study of Saudi Arabia*. Applied Energy, 2017. **185**: 410-420.
51. Ariunbaatar, J., A. Panico, G. Esposito, F. Pirozzi, and P.N.L. Lens, *Pretreatment methods to enhance anaerobic digestion of organic solid waste*. Applied Energy, 2014. **123**: 143-156.
52. Zhao, Z., Y. Zhang, D.E. Holmes, Y. Dang, T.L. Woodard, K.P. Nevin, and D.R. Lovley, *Potential enhancement of direct interspecies electron transfer for syntrophic metabolism of propionate and butyrate with biochar in up-flow anaerobic sludge blanket reactors*. Bioresource Technology, 2016. **209**: 148-156.
53. Lei, Y., D. Sun, Y. Dang, H. Chen, Z. Zhao, Y. Zhang, and D.E. Holmes, *Stimulation of methanogenesis in anaerobic digesters treating leachate from a municipal solid waste*

*incineration plant with carbon cloth*. Bioresource technology, 2016. **222**: 270-276.

54. Zhao, Z., Y. Zhang, T. Woodard, K. Nevin, and D. Lovley, *Enhancing syntrophic metabolism in up-flow anaerobic sludge blanket reactors with conductive carbon materials*. Bioresource technology, 2015. **191**: 140-145.

## List of Figures and Tables

Fig.1. Schematic diagram of the AMPTS II system for batch anaerobic digestion experiments.

Fig. 2. Effects of graphene addition on biomethane production from mesophilic anaerobic digestion: (a) biomethane yield, and (b) biomethane production rate.

Fig. 3. Effects of graphene addition on biomethane production from thermophilic anaerobic digestion: (a) biomethane yield, and (b) biomethane production rate.

Fig. 4. Effects of graphene addition on ethanol and acetate conversion in (a) mesophilic anaerobic digestion, and (b) thermophilic anaerobic digestion.

Fig. 5. Proposed microbial networks of key bacteria and archaea for ethanol degradation with graphene addition in (a) mesophilic and (b) thermophilic anaerobic digestion (the numbers in brackets indicate the abundance of microorganisms).

Table 1 Kinetic parameters of biomethane production in mesophilic and thermophilic anaerobic digestion with/without graphene addition.

Table 2 Changes in Gibbs free energy values for ethanol conversion to methane at different temperatures.

Table 3 Richness and diversity statistics of bacterial and archaeal community in mesophilic and thermophilic anaerobic digestion with/without graphene addition.

Table 4 Bacterial community composition and diversity after mesophilic and thermophilic digestion.

Table 5 Archaeal community composition and diversity after mesophilic and thermophilic digestion.

Table 6 A summary of typical carbon-based materials on the performance of mesophilic and thermophilic digestion in literature.

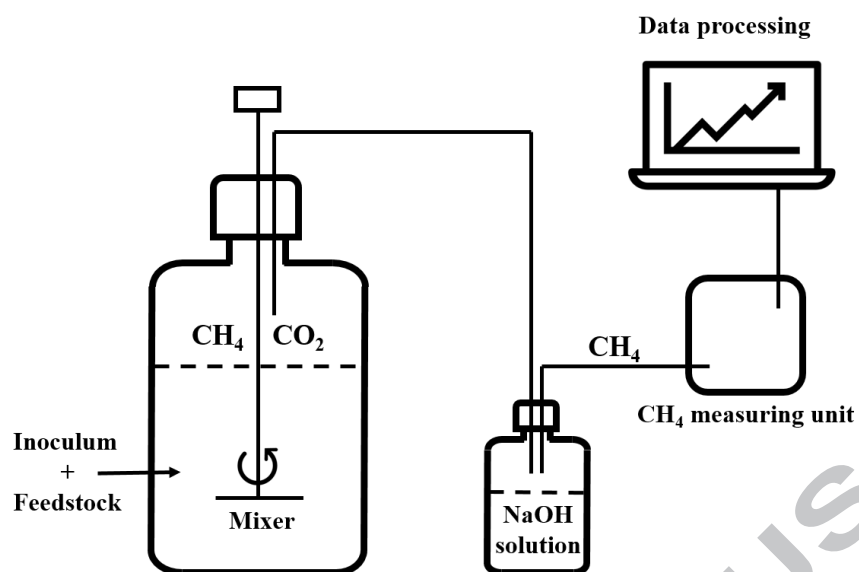


Fig.1. Schematic diagram of the AMPTS II system for batch anaerobic digestion experiments.

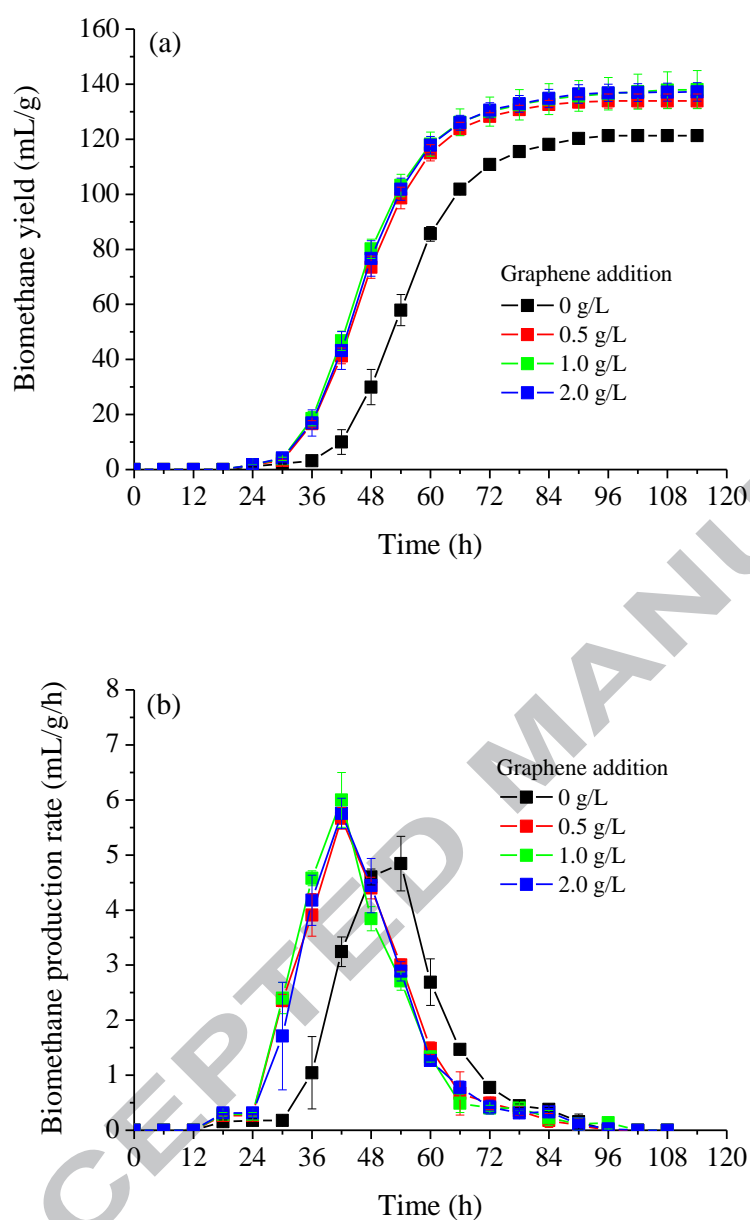


Fig. 2. Effects of graphene addition on biomethane production from mesophilic anaerobic digestion: (a)

biomethane yield, and (b) biomethane production rate.

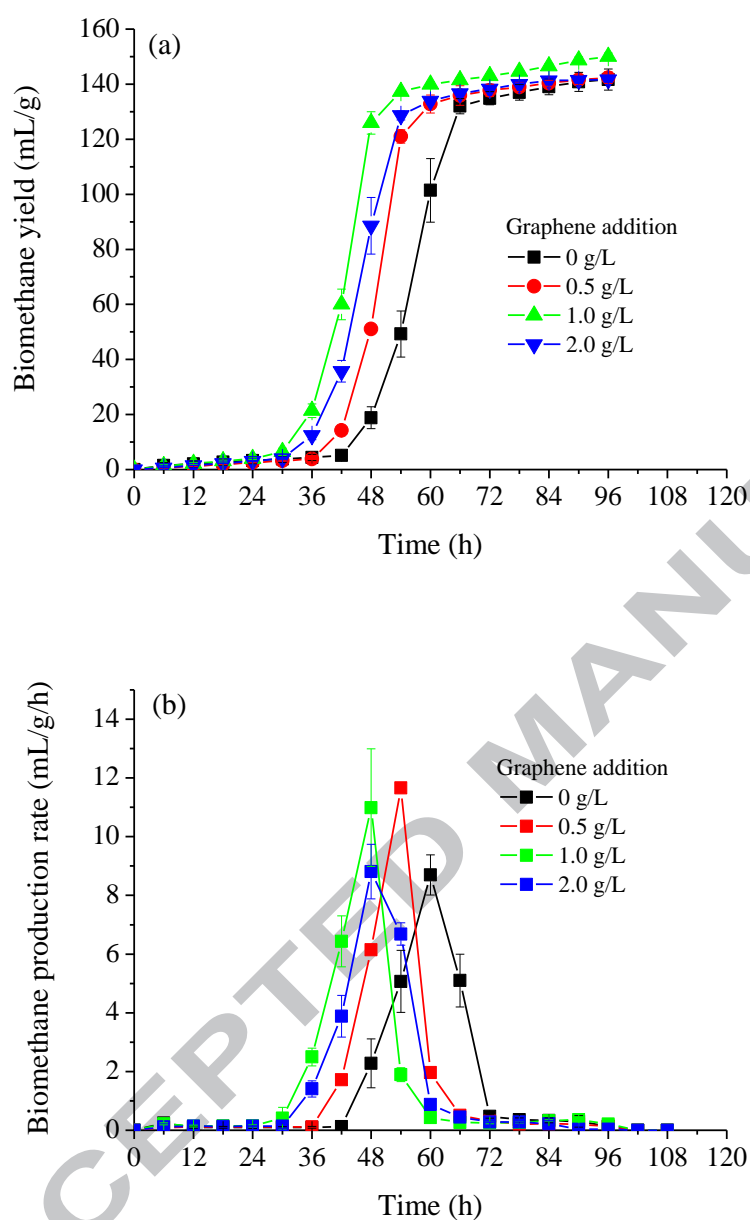


Fig. 3. Effects of graphene addition on biomethane production from thermophilic anaerobic digestion:

(a) biomethane yield, and (b) biomethane production rate.

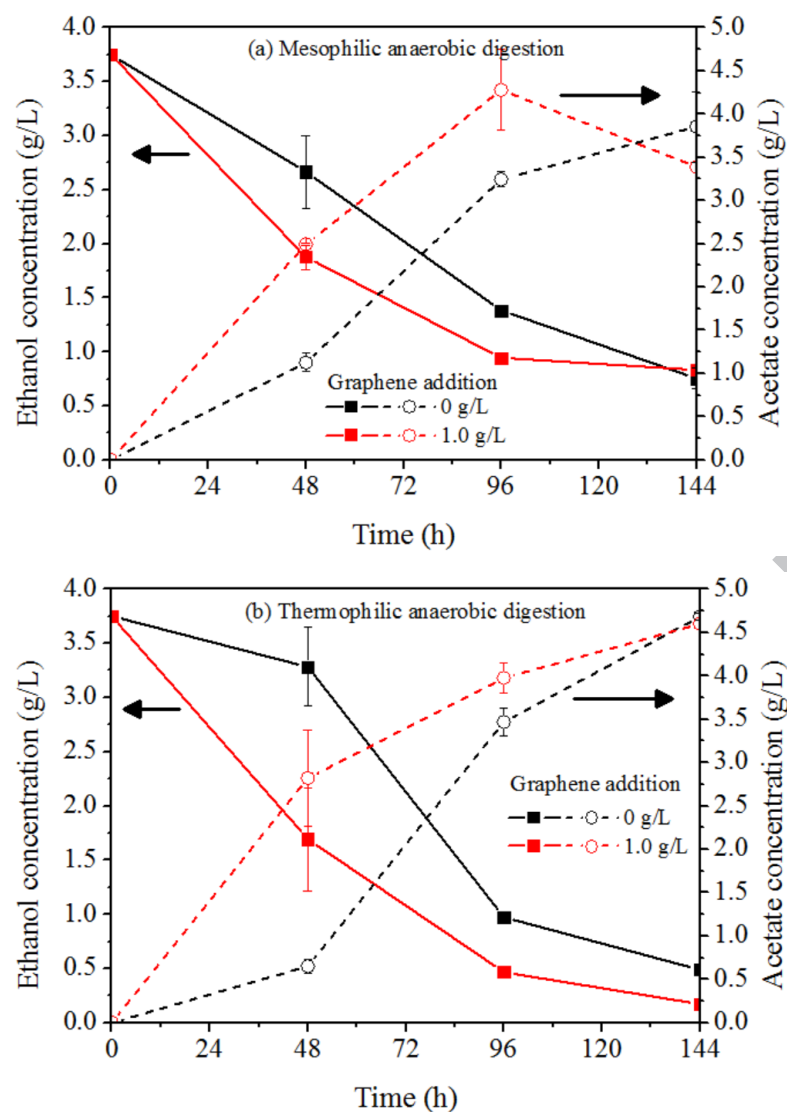


Fig. 4. Effects of graphene addition on ethanol and acetate conversion in (a) mesophilic anaerobic digestion, and (b) thermophilic anaerobic digestion.



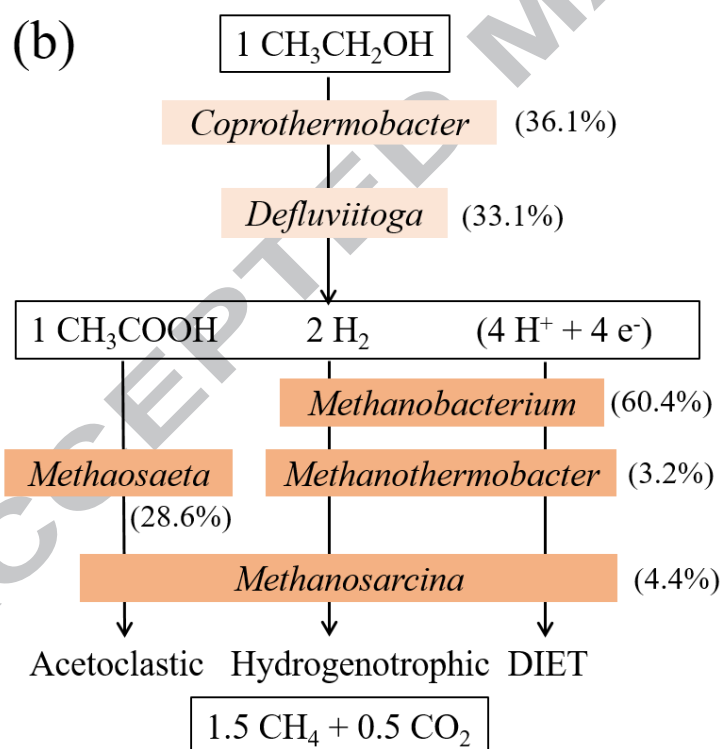
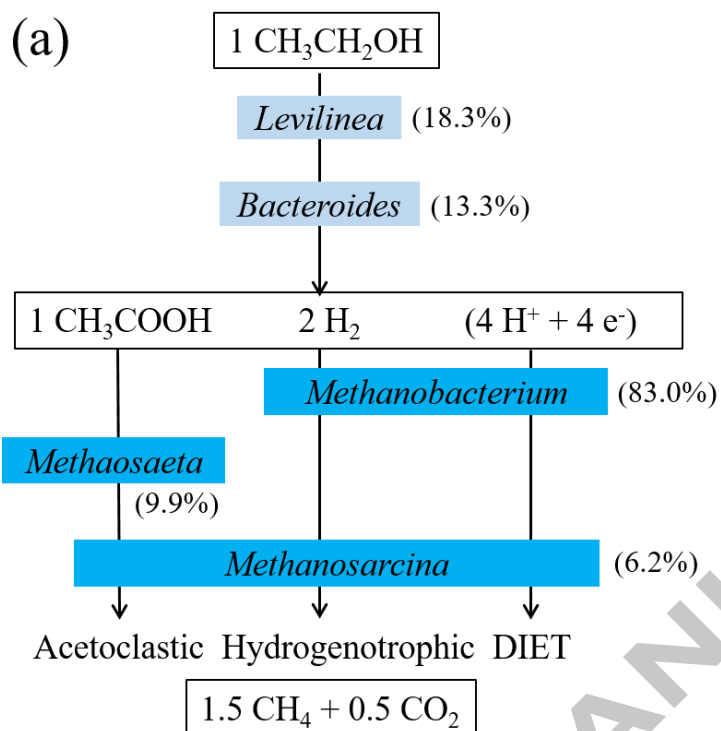


Fig. 5. Proposed microbial networks of key bacteria and archaea for ethanol degradation with graphene

addition in (a) mesophilic and (b) thermophilic anaerobic digestion (the numbers in brackets indicate

the abundance of microorganisms).

Table 1 Kinetic parameters of biomethane production in mesophilic and thermophilic anaerobic

digestion with/without graphene addition.

Digestion type	Graphene addition (g/L)	Kinetic model parameters				
		$H_m$ (mL/g)	$R_m$ (mL/g/d)	$\lambda$ (d)	$T_m$ (d)	$R^2$
Mesophilic	0	121.8	4.9	41.9	51.0	0.9996
	0.5	134.2	5.3	34.0	43.3	0.9998
	1.0	136.9	5.4	33.2	42.5	0.9955
	2.0	137.0	5.5	33.8	43.0	0.9999
Thermophilic	0	141.7	8.6	47.5	53.6	0.9958
	0.5	139.7	14.4	44.3	47.9	0.9957
	1.0	146.1	9.4	35.7	41.4	0.9960
	2.0	141.0	9.5	38.0	43.5	0.9968

$H_m$ : maximum biomethane yield potential,  $R_m$ : peak biomethane production rate,  $\lambda$ : lag-phase time, and

$T_m$ : peak time.

Table 2 Changes in Gibbs free energy values for ethanol conversion to methane at different temperatures.

Microbes	Reactions	$\Delta G^{0ra}$ (kJ/mol)		
		25 °C <sup>b</sup>	35 °C <sup>c</sup>	55 °C <sup>d</sup>
Electron producing acidogen	1. MIET: $\text{CH}_3\text{CH}_2\text{OH} + \text{H}_2\text{O} \rightarrow \text{CH}_3\text{COO}^- + \text{H}^+ + 2\text{H}_2$	9.7	10.4	12.3
	2. DIET: $\text{CH}_3\text{CH}_2\text{OH} + \text{H}_2\text{O} \rightarrow \text{CH}_3\text{COO}^- + 5\text{H}^+ + 4\text{e}^-$	-149.6	-151.4	-152.9
Electron consuming methanogen	3. MIET: $2\text{H}_2 + 1/2\text{CO}_2 \rightarrow 1/2\text{CH}_4 + \text{H}_2\text{O}$	-65.4	-66.1	-67.2
	4. DIET: $4\text{H}^+ + 4\text{e}^- + 1/2\text{CO}_2 \rightarrow 1/2\text{CH}_4 + \text{H}_2\text{O}$	94.0	95.7	98.0
Overall	5. $\text{CH}_3\text{CH}_2\text{OH} + 1/2\text{CO}_2 \rightarrow 1/2\text{CH}_4 + \text{CH}_3\text{COO}^- + \text{H}^+$	-55.7	-55.7	-54.8

<sup>a</sup> Values are calculated at different temperatures under standard conditions (1 M concentration of all solutes, 1 atm, and neutral pH). Negative value indicates the reaction is thermodynamically favorable and proceeds spontaneously.

<sup>b</sup> Based on values tabulated by Thauer et al. [28].

<sup>c</sup> Based on values at actual temperature of 37 °C tabulated by Amend and Shock [27].

<sup>d</sup> Based on values tabulated by Amend and Shock [27].

Table 3 Richness and diversity statistics of bacterial and archaeal community in mesophilic and thermophilic anaerobic digestion with/without graphene addition.

Digestion type	Sample	Bacterial community				Archaeal community			
		OTUs <sup>a</sup>	Chao <sup>b</sup>	Shannon <sup>c</sup>	Coverage <sup>d</sup>	OTUs	Chao	Shannon	Coverage
Mesophilic	Original inoculum	853	1081	4.25	0.99	96	157	1.36	1.00
	Graphene 0	676	900	4.05	0.99	74	118	0.91	1.00
	Graphene 1	734	1021	4.30	0.99	66	98	1.05	1.00
Thermophilic	Original inoculum	525	779	3.35	0.99	150	196	1.98	1.00
	Graphene 0	441	586	2.23	0.99	145	182	1.94	1.00
	Graphene 1	467	692	2.40	0.99	148	217	2.04	1.00

Graphene 0: sample for digestate without graphene addition. Graphene 1: sample for digestate with 1.0 g/L of graphene addition.

<sup>a</sup> OTUs were identified based on a 97% sequence similarity.

<sup>b</sup> Chao richness estimator: the total number of OTUs estimation by infinite sampling. A higher number indicates higher richness.

<sup>c</sup> Shannon's diversity index: an index to characterize species diversity. A higher value indicates more diversity.

<sup>d</sup> Good's coverage: estimated probability that the next read will belong to an OUT that has already been found.

Table 4 Bacterial community composition and diversity after mesophilic and thermophilic digestion.

Genera	Mesophilic anaerobic digestion			Thermophilic anaerobic digestion		
	Original inoculum	Graphene 0	Graphene 1	Original inoculum	Graphene 0	Graphene 1
<i>Levilinea</i>	18.4	29.0	18.3	0.3	0.1	0.1
<i>Coprothermobacter</i>	0.0	0.1	0.0	27.0	44.8	36.1
<i>Defluviitoga</i>	0.0	0.5	0.2	7.9	26.9	33.3
<i>Bacteroides</i>	12.7	5.9	13.3	0.0	0.0	0.0
<i>Acinetobacter</i>	3.7	0.8	1.1	16.3	1.3	0.7
<i>Clostridium III</i>	3.3	0.6	4.8	11.9	5.7	7.2
<i>Sedimentibacter</i>	1.2	3.2	2.1	0.1	0.0	0.0
<i>Clostridium XIVa</i>	5.9	1.9	4.8	0.5	0.3	0.4
<i>Aminivibrio</i>	0.9	3.8	2.2	0.2	0.1	0.0
<i>Exiguobacterium</i>	0.6	2.1	1.0	0.7	3.1	1.4
unclassified	10.6	15.2	16.3	5.5	1.6	1.6
Others	42.7	36.8	35.9	29.6	16.2	19.3

Graphene 0: sample for digestate without graphene addition, Graphene 1: sample for digestate with 1.0 g/L of graphene addition.

Table 5 Archaeal community composition and diversity after mesophilic and thermophilic digestion.

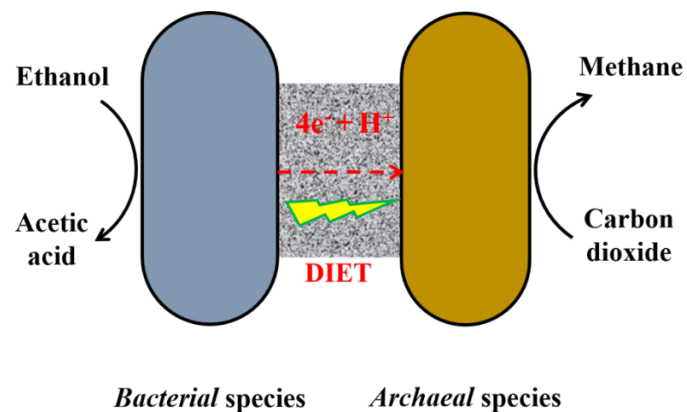
Genera	Mesophilic anaerobic digestion			Thermophilic anaerobic digestion		
	Original inoculum	Graphene 0	Graphene 1	Original inoculum	Graphene 0	Graphene 1
<i>Methanobacterium</i>	64.3	88.8	83.0	39.8	52.8	60.4
<i>Methanosaeta</i>	27.2	8.4	9.9	26.1	38.2	28.6
<i>Methanosarcina</i>	6.0	2.6	6.2	30.1	5.7	4.4
<i>Methanomassiliicoccus</i>	0.9	0.0	0.6	0.1	0.3	1.1
<i>Methanospirillum</i>	1.5	0.2	0.2	0.5	0.2	0.1
<i>Methanothermobacter</i>	0.0	0.0	0.0	0.0	1.9	3.2
unclassified	0.1	0.0	0.0	0.0	0.0	0.4
Others	0.2	0.0	0.1	3.4	1.0	1.9

Graphene 0: sample for digestate without graphene addition, Graphene 1: sample for digestate with 1.0 g/L of graphene addition.

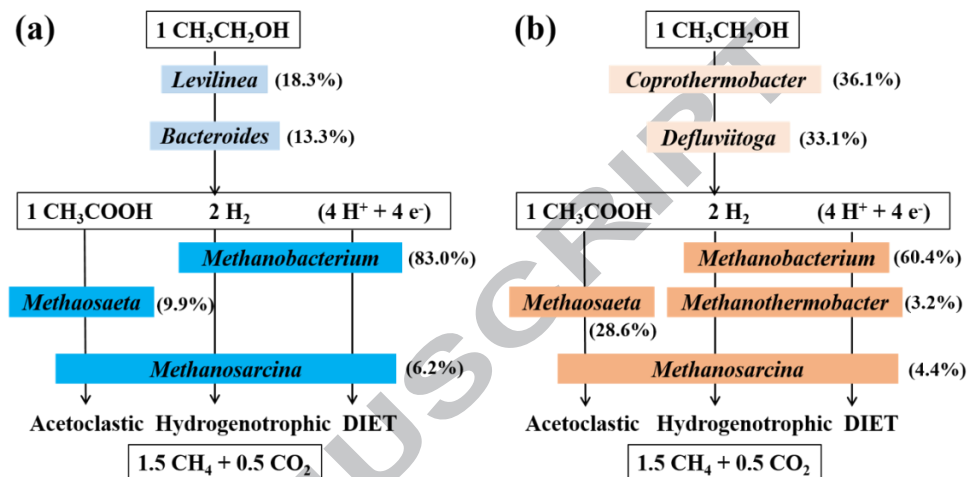
Table 6 A summary of typical carbon-based materials on the performance of mesophilic and thermophilic digestion in literature.

Conductive material	Substrate	Temperature (°C)	Reactor configuration	Methane production rate increase	Reference
Biochar	Propionate/butyrate	37	UASB	16-25%	[52]
Carbon cloth	MSW leachate	33	UASB	29.2%	[53]
Carbon cloth, graphite, and biochar	Ethanol	37	UASB	30-45%	[54]
GAC	Propionate/butyrate	37	Batch	12-30%	[49]
GAC	Acetate	35	CSTR	77.6%	[22]
Carbon nanotube	Sucrose	35	Batch	100%	[36]
Graphene	Glucose	35	Batch	17-51.4%	[29]
Graphene	Ethanol	35	Batch	20.0%	[25]
GAC	Glucose	55	Batch	1.9%	[10]
Carbon nanotube	Glucose	55	Batch	13.9%	[10]
Graphene	Ethanol	35	Batch	25.0%	This study
Graphene	Ethanol	55	Batch	26.4%	This study

GAC: granular activated carbon, MSW: municipal solid waste, UASB: up-flow anaerobic sludge blanket, CSTR: continuous stirred-tank reactor.



Graphene-based DIET in mesophilic and thermophilic anaerobic digestion



Microbial networks for ethanol degradation in (a) mesophilic and (b) thermophilic digestion



## Highlights

Graphene enhanced mesophilic and thermophilic anaerobic digestion (MAD, TAD) by ~25%.

Potential direct interspecies electron transfer (DIET) was established via graphene.

DIET fluxes in MAD and TAD were at similar level (76.4 vs 75.1 mA).

Diverse temperature-dependent bacteria and archaea might participate in DIET.